Insufficiency of Pro-heparin-binding Epidermal Growth Factor-like Growth Factor Shedding Enhances Hypoxic Cell Death in H9c2 Cardiomyoblasts via the Activation of Caspase-3 and c-Jun N-terminal Kinase*[S]

Teruyoshi Uetani[‡§], **Hironao Nakayama**[‡], **Hideki Okayama**[§], **Takafumi Okura**[§], **Jitsuo Higaki**[§], **Hirofumi Inoue**[‡1], and **Shigeki Higashiyama**[‡¶]

From the Departments of [‡]*Biochemistry and Molecular Genetics and* [§]*Integrated Medicine and Informatics and* [¶]*Protein Network Laboratory, Center for Regenerative Medicine (CEREM), Ehime University, Graduate School of Medicine, Shitsukawa, Toon, Ehime 791-0295, Japan*

Heparin-binding epidermal growth factor-like growth factor (HB-EGF) is a cardiogenic and cardiohypertrophic growth factor. ProHB-EGF, a product of the *Hb-egf* gene and the precursor of HB-EGF, is anchored to the plasma membrane. Its ectodomain region is shed by a disintegrin and metalloproteases (ADAMs) when activated by various stimulations. It has been reported that an uncleavable mutant of *Hb-egf, uc-Hb-egf,* produces uc-proHB-EGF, which is not cleaved by ADAMs and causes dilation of the heart in knock-in mice. This suggests that the shedding of proHB-EGF is essential for the development and survival of cardiomyocytes: however, the molecular mechanism involved has remained unclear. In this study, we investigated the relationship between uc-proHB-EGF expression and cardiomyocyte survival. Human uc-proHB-EGF was adenovirally introduced into the rat cardiomyoblast cell line H9c2, and the cells were cultured under normoxic and hypoxic conditions. Uc-proHB-EGF-expressing H9c2 cells underwent apoptosis under normoxic conditions, which distinctly increased under hypoxic conditions. Furthermore, we observed an increased Caspase-3 activity, reactive oxygen species accumulation, and an increased c-Jun N-terminal kinase (JNK) activity in the uc-proHB-EGF-expressing H9c2 cells. Treatment of the uc-proHB-EGF transfectants with inhibitors of Caspase-3, reactive oxygen species, and JNK, namely, Z-VAD-fmk, *N*-acetylcysteine, and SP600125, respectively, significantly reduced hypoxic cell death. These data indicate that insufficiency of proHB-EGF shedding under hypoxic stress leads to cardiomyocyte apoptosis via Caspase-3- and JNK-dependent pathways.

One of the cardiogenic and cardiohypertrophic growth factors is the heparin-binding epidermal growth factor-like growth factor (HB-EGF),[2] which is a member of the EGF family

(1, 2). An up-regulated *Hb-egf* expression is observed under conditions of tissue damage, hypoxia, and oxidative stress. The preventive roles of HB-EGF against hypoxia-induced apoptosis have been focused upon with regard to various organs, including the intestine (3–5), kidney (6, 7), skeletal muscle (8), brain (9, 10), placenta (11), and heart (12). Furthermore, it has also been demonstrated that the expression levels of *Hb-egf* and EGF receptor (EGFRs) mRNAs significantly increased in tissues surrounding myocardial infarction lesions (13, 14).

HB-EGF is synthesized as a type I transmembrane protein (proHB-EGF) (1). Following ectodomain shedding, which is the cleavage of the juxtamembrane domain from the membrane-anchored protein, by a disintegrin and metalloprotease (ADAM) and matrix metalloprotease, a soluble form of *Hb-egf* product (HB-EGF) is released into the extracellular space and binds to the EGFRs (15, 16). The EGFRs bound to HB-EGF become phosphorylated and activate downstream signaling of the receptors such as mitogen-activated protein kinase and phosphatidylinositol 3-kinase. On the other hand, the C-terminal fragment of proHB-EGF (HB-EGF-CTF) translocates to the inner nuclear membrane and regulates the transcriptional activity by releasing transcriptional repressors such as promyelocytic leukemia zinc finger protein and B-cell lymphoma/leukemia-6 protein (Bcl-6) from DNA (17–19).

ProHB-EGF shedding itself has been known to play an important role in proliferation, differentiation, and survival of various types of cells. It has been reported that mice expressing an uncleavable proHB-EGF (uc-proHB-EGF) mutant (HB[uc/uc]) develop severe cardiac dilation, which is not observed in proHB-EGF null mice (20, 21). Histological examination of the hearts of the HB[uc/uc] mice revealed loss of cardiomyocytes, which is similar to that found in ischemic or idiopathic dilated

[S] The on-line version of this article (available at http://www.jbc.org) contains supplemental Figs. S1–S3 and Table S1.
[1] To whom correspondence should be addressed. Tel.: 81-89-960-5254; Fax: 81-89-960-5256; E-mail: hinoue66@m.ehime-u.ac.jp.
[2] The abbreviations used are: HB-EGF, heparin-binding epidermal growth factor-like growth factor; proHB-EGF, a precursor of HB-EGF; wt, wild type; uc,

uncleavable form; GFP, green fluorescent protein; ADAM, a disintegrin and metalloproteases; JNK, c-Jun N-terminal kinase; ROS, reactive oxygen species; Bcl, B-cell lymphoma/leukemia; TAK1, transforming growth factor-β-activated kinase 1; BAG-1, Bcl-2-associated athanogene-1; fmk, fluoromethyl ketone; Z, benzyloxycarbonyl; DCFDA, 5-(and -6)-carboxy-2′,7′-dichlorodihydrofluorescein diacetate; ERK1/2, extracellular signal-regulated kinase 1/2; XIAP, X-linked inhibitor of apoptosis; ASK1, apoptosis signal-regulating kinase 1; EGFR, epidermal growth factor receptor; CTF, C-terminal fragment; NAC, *N*-acetylcysteine; FITC, fluorescein isothiocyanate; siRNA, small interfering RNA.

cardiomyopathy. It has also been demonstrated that proHB-EGF shedding is required for human trophoblast survival under hypoxic conditions (11). However, the molecular mechanism underlying tissue disturbance that depends on impaired proHB-EGF shedding remains unclear.

In this study, we investigated the role of proHB-EGF shedding in the survival of a rat cardiomyoblast cell line, H9c2. Overexpression of uc-proHB-EGF or abrogation of proHB-EGF shedding by a metalloprotease inhibitor enhanced cell death both under normoxic and hypoxic conditions. However, the effect was considerably more under hypoxic conditions. Furthermore, we found that uc-proHB-EGF caused the activation of Caspase-3 and c-Jun N-terminal kinase (JNK) as well as the accumulation of reactive oxygen species (ROS). Our findings would be helpful in understanding the molecular mechanisms involved in the survival of cardiomyoblasts under hypoxic conditions and determination of the local HB-EGF concentration in coronary arteries may be useful in developing a novel prognostic marker in ischemic heart disease.

EXPERIMENTAL PROCEDURES

Reagents—Recombinant human HB-EGF and Z-VAD-fmk were purchased from R&D Systems and MBL, respectively. SP600125 and *N*-acetylcysteine (NAC) were purchased from Sigma. KB-R7785 and KB-R10082 were gifts from Carna Biosciences Inc. 5-(and -6)-Carboxy-2′,7′-dichlorodihydrofluorescein diacetate (DCFDA) was purchased from Invitrogen.

Cell Culture—Rat embryonic cardiomyoblasts H9c2 were purchased from the American Tissue Culture Collection (ATCC: CRL-1446) and cultured in Dulbecco's modified Eagle's medium (Nikken) supplemented with 10% fetal calf serum, 100 units/ml penicillin, and 100 μg/ml streptomycin (Meiji) in a humidified incubator with 5% CO_2 at 37 °C.

Adenovirus Construction and Infection—Adenovirus vectors carrying genes encoding green fluorescent protein (GFP), LacZ, wild-type proHB-EGF (wt-proHB-EGF), and uc-proHB-EGF were constructed using an adenovirus expression kit (Takara Bio Inc.). The cells were infected with purified, concentrated, and titer-checked viruses at a multiplicity of infection of 40 for 6 h before subjection to hypoxic conditions.

Simulated Ischemia Model—Hypoxic conditions were created using a chamber with Anaero-Pack (Mitsubishi Gas Chemical), which catalytically reduced O_2 concentration to 1% within 60 min at 37 °C. After the adenoviral infection, the cells were cultured in the hypoxic chamber for the indicated time periods.

Immunoblotting—Cell lysates were immunoblotted according to a previously described method (19). The primary antibodies used in this study were as follows: rabbit polyclonal antibody against EGFR, Bax (Santa Cruz Biotechnology), phosphotyrosine (Upstate Biotechnology), JNK, phospho-JNK, p38, phospho-p38, Akt, phospho-Akt, extracellular signal-regulated kinase 1/2 (ERK1/2), phospho-ERK1/2 (Cell Signaling Technology), Bcl-XL, Caspase-3 (Abcam), proHB-EGF (H1) (19), mouse monoclonal antibody against β-actin (Sigma), and goat polyclonal antibody against *X*-linked inhibitor of apoptosis (XIAP; R&D Systems). After incubation with the abovementioned primary antibodies, the membranes were incubated for

1 h with secondary antibodies, namely, horseradish peroxidase-conjugated anti-mouse, anti-rabbit, or anti-goat immunoglobulin (Promega).

Trypan Blue Dye Exclusion Assay—Monolayer cells were rinsed with phosphate-buffered saline and treated with trypsin and EDTA. They were then immediately stained with 0.5% typan blue. Cell viability was determined by counting the unstained cells under a microscope.

Terminal Deoxynucleotidyl Transferase-mediated dUTP Nick End-labeling (TUNEL) Assay—TUNEL staining was performed using a commercially available kit (ApopTag fluorescein *in situ* apoptosis detection kit; Chemicon) according to the manufacturer's instructions. The extent of binding of a fluorescent antibody to digoxigenin in the positive cells was determined by observing under a fluorescent microscope.

Measurement of Caspase-3 Activity—The activity of Caspase-3 was measured by the cleavage of a Caspase-3 substrate, FAM-DEVD-fmk, using a commercially available kit (Apo LOGIX Carboxyfluorescein Caspase detection kit; Cell Technology Inc.).

Fluorescein Isothiocyanate (FITC)-labeled Annexin V (Annexin V-FITC) Assay—Apoptosis was detected using a commercially available kit (Annexin V-FITC kit; Beckman Coulter) in accordance with the protocol provided by the manufacturer. Detection of Annexin V positive cells was performed by an Olympus fluorescent microscopy or FACSCalibur (BD Bioscience).

Alkaline Phosphatase-ProHB-EGF Shedding Assay—H9c2 cells stably expressing alkaline phosphatase-tagged proHB-EGF were cloned. The cells were treated with KB-R7785 or KB-R10082 (final 10 μM) and phorbol 12-myristate 13-acetate (final 100 nM) for 1 h. Aliquots (100 μl each) of the conditioned media were used to measure alkaline phosphatase activity as described previously (22).

Live Cell Imaging—The cells were cultured in glass-bottomed dishes and observed using BioStation IM (Nikon). The phase-contrast images were acquired every 20 min for 60 h.

Evaluation of ROS Accumulation—Oxidative stress was evaluated by measuring the intracellular generation of H_2O_2. The cells were seeded in 96-well plates. After subjection to hypoxic conditions for 24 h, the cells were incubated in the dark for 30 min with 20 μM DCFDA. Dichlorofluorescein (DCF) fluorescence was measured using a multiplate fluorometer (Wallac ARVO SX; PerkinElmer Life Sciences) at excitation and emission wavelengths of 488 and 530 nm, respectively. The DCF images were also obtained by a fluorescence microscopy (Olympus).

RT² Profiler PCR Array System—The expression of 84 apoptosis-related genes in a rat were examined using the RT² Profiler PCR array (SuperArray Bioscience). Total RNA was isolated from the GFP- or uc-proHB-EGF-expressed H9c2 cells (GFP/H9c2 or uc-proHB-EGF/H9c2) by using the TRIzol reagent (Invitrogen) and RNeasy mini kit (Qiagen). cDNA was synthesized from 1 μg of RNA using a SuperScript RT II enzyme (Invitrogen). PCR was performed with the RT² Profiler PCR array system according to the manufacturer's instructions using ABI 7300 (Applied Biosystems). The expression levels of the mRNA of each gene in uc-proHB-EGF/H9c2 were normal-

ized using the expression of *Rplp1, Hprt1, Rpl13a, Ldha*, and *Actb*, considered the housekeeping genes and then compared with the data obtained from GFP/H9c2. The results were confirmed by quantitative reverse transcriptase-PCR performed using individual RNA samples from the cells in each group by LightCycler (Roche Applied Science). The primers used for real-time PCR are listed in supplemental Table S1.

Gene Knockdown Assay—Small interference RNA (siRNA) against *Hb-egf*, *JNK*, and *Caspase-3* were purchased from Applied Biosystems Inc. The siRNA was transfected by Code-Breaker™ siRNA transfection reagent (Promega) at 40 nM following the instruction manual, and the transfectants were infected by the adenoviruses at 24 h after transfection. Six hours later, the cells were incubated under hypoxia for 36 h. The knockdown efficiency of each was validated by a TaqMan gene expression assay (Applied Biosystems) or Western blotting. The siRNA used for a knockdown assay are listed in supplemental Table S1.

Statistical Analysis—All assays were independently performed 3 times. The results are represented as mean ± S.E. The 2 groups were compared using the Student's *t* test. Analysis of variance with Bonferroni post hoc test was used for multiple comparisons. $p < 0.05$ was considered statistically significant.

RESULTS

Overexpression of Uc-proHB-EGF in H9c2 Cells Increased Cell Death under Normoxic Conditions—To investigate the functional role of proHB-EGF shedding in cardiomyocyte survival, rat cardiomyoblasts H9c2 were infected with adenovirus carrying cDNA of GFP, wt-proHB-EGF, or uc-proHB-EGF, and each group of the cells were cultured under normoxic conditions. The infected cells were sequentially observed under a microscope. Time-lapse imaging showed no difference in cell viability among the cells in the 3 groups for the first 36 h (Fig. 1*A*, supplemental Fig. S1*A*). However, at 42 h after the infection, uc-proHB-EGF/H9c2 began to die (data not shown). Blebbing, one of the phenomena observed during apoptosis, was also observed in uc-proHB-EGF/H9c2. At 48 h, the viability of uc-proHB-EGF/H9c2 decreased by ~30% as compared with the viabilities of the other cells (Fig. 1*B*, supplemental Fig. S1*B*).

The Uc-proHB-EGF/H9c2 Apoptosis Was Enhanced under Hypoxic Conditions—Hypoxia is a pathophysiological condition frequently occurring in cardiomyocytes. To investigate the effect of uc-proHB-EGF on cell death under hypoxic stress, we cultured uc-proHB-EGF/H9c2 under hypoxic conditions. Apoptosis developed more significantly and promptly in uc-proHB-EGF/H9c2 than in the cells of other groups (Fig. 1, *A*, *C*, and *D*). The TUNEL and Annexin V-FITC assays also revealed a significant enhancement of apoptosis in uc-proHB-EGF/H9c2 at 36 h after hypoxia (Fig. 1, *E* and *F*). Furthermore, the uc-proHB-EGF-enhanced cell death was not recovered by co-expression of wt-proHB-EGF (Fig. 1*G*). Next, we performed the assay with H9c2 cells treated with siRNA against *Hb-egf*. The expression of *Hb-egf* in knockdown cells decreased to apparently 30% in the mRNA level (*box* in Fig. 1*H*). However, knockdown of *Hb-egf* had no effect on hypoxia-induced apoptosis (Fig. 1*H*). These data indicate that proHB-EGF shedding

but not its expression is associated with survival of cardiomyocytes under hypoxia.

The Released HB-EGF Did Not Regulate H9c2 Cell Viability under Hypoxia—To confirm that sufficient proHB-EGF shedding is important to maintain cell viability under hypoxic conditions, we used an ADAM inhibitor, KB-R7785, in cell culture. KB-R7785 has been established as an effective inhibitor of proHB-EGF shedding *in vivo* and *in vitro* (23). To examine whether KB-R7785 also works as an inhibitor of proHB-EGF shedding in H9c2 cells, we performed an alkaline phosphatase-proHB-EGF shedding assay with a stable H9c2 transfectant with alkaline phosphatase-tagged proHB-EGF. The result showed that shedding of proHB-EGF by phorbol 12-myristate 13-acetate, a strong inducer of proHB-EGF shedding (24), was completely blocked by KB-R7785 (supplemental Fig. S2). On the other hand, KB-R10082, an inactive analog of KB-R7785, had no effect on the shedding. We sequentially investigated effects of these compounds on apoptosis of H9c2 cells under hypoxia. In the presence of KB-R7785, the viabilities of mock/H9c2, GFP/H9c2, and wt-proHB-EGF/H9c2 significantly decreased under hypoxic conditions. However, the viability of uc-proHB-EGF/H9c2 remained unaffected (Fig. 2, *A* and *B*). KB-R10082 had no apparent effect on the apoptosis induction under hypoxic conditions. ProHB-EGF shedding results in paracrine and/or autocrine manners of HB-EGF. To investigate whether the enhancement of apoptosis is due to the reduced production of HB-EGF in uc-proHB-EGF/H9c2, recombinant human HB-EGF was added to the cell culture. Recombinant HB-EGF could not adequately recover the viability of uc-proHB-EGF/H9c2, although tyrosine phosphorylation of EGFR by recombinant HB-EGF was observed in uc-proHB-EGF/H9c2, as well as in GFP/H9c2 or wt-proHB-EGF/H9c2 (Fig. 2, *C–E*).

Caspase-3-dependent Pathway Played a Part in Cell Death by Uc-proHB-EGF Expression—The activity of a unique class of cysteine proteases called Caspases is involved in effecting cell death. To investigate the involvement of Caspases-dependent pathways in the uc-proHB-EGF/H9c2 apoptosis, we examined the activity of Caspase-3, the final executor of apoptosis, in uc-proHB-EGF/H9c2 exposed to hypoxic conditions. Caspase-3 activity increased more significantly in uc-proHB-EGF/H9c2 than in the cells of other groups (Fig. 3, *A* and *B*). Moreover, we observed the inhibitory effect of a pan-Caspase inhibitor, Z-VAD-fmk, on uc-proHB-EGF/H9c2 apoptosis. Although Z-VAD-fmk strongly inhibited Caspase-3 activity, it failed to completely recover the cells from apoptosis (Fig. 3, *A–D*). These results suggest that not only Caspase-dependent but also Caspase-independent pathways are involved in this effecting cell death.

ROS Accumulated in Uc-proHB-EGF/H9c2 under Hypoxic Conditions, and a ROS Scavenger Reduced the Enhanced Cell Death—Hypoxia increases mitochondrial ROS generation at Complexes I and III (25–28). Moreover, ROS has been known as a proapoptotic factor that activates stress-activated protein kinases. We evaluated the accumulation of ROS in each of the gene transfectants under hypoxic conditions. The results showed that the level of ROS accumulation was higher in uc-proHB-EGF/H9c2 than in the cells of the other groups (Fig.

A

* p<0.05% vs other groups

B

C

D

* p<0.05% vs other groups

E

F

* p<0.05% vs other groups

G

H
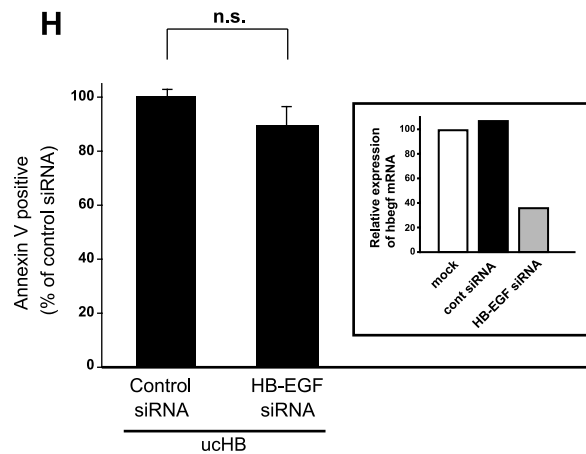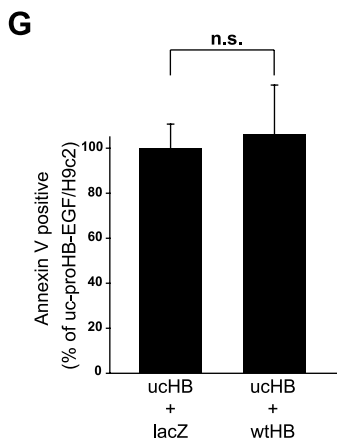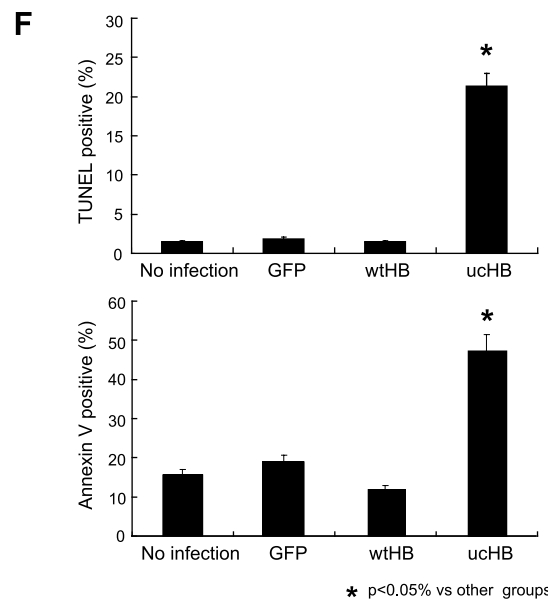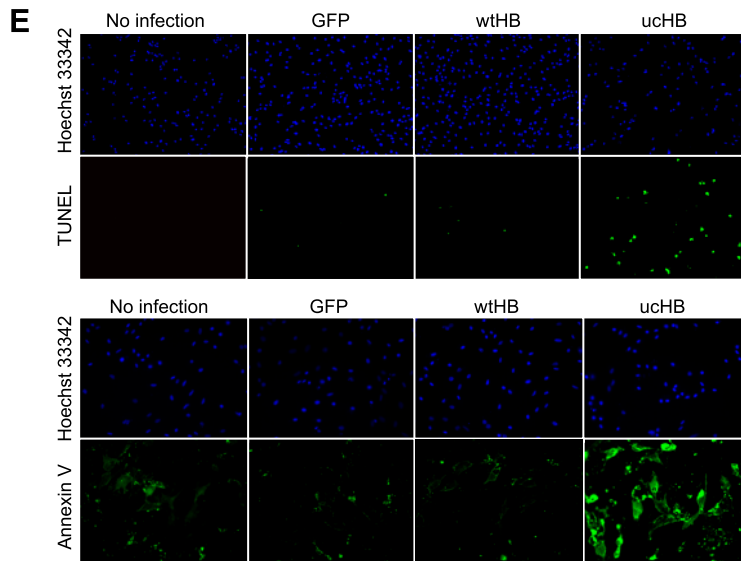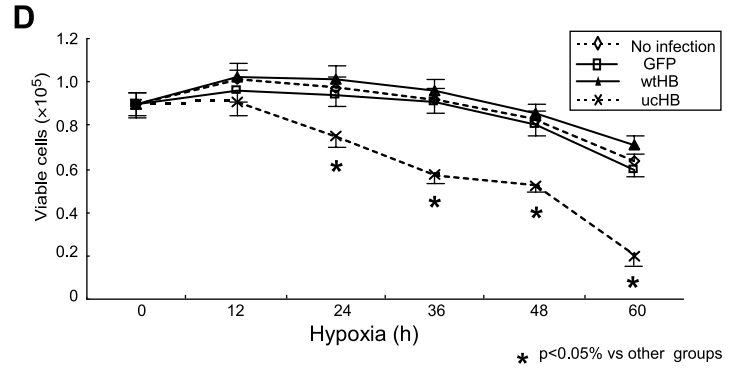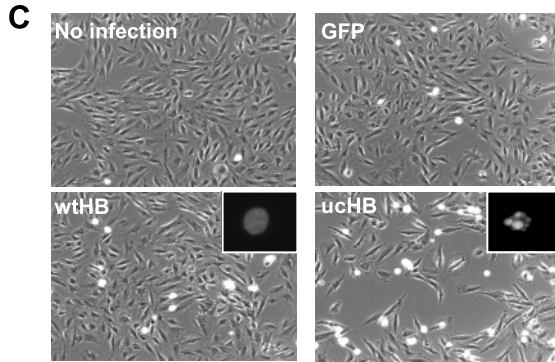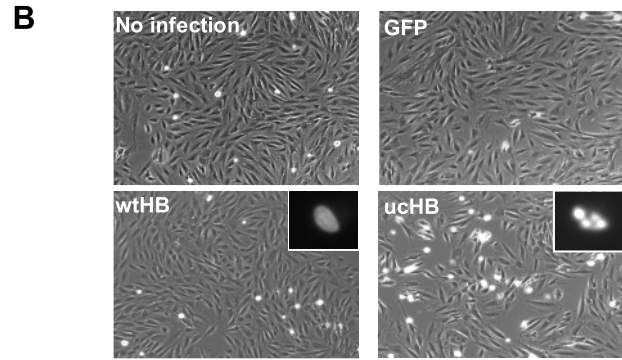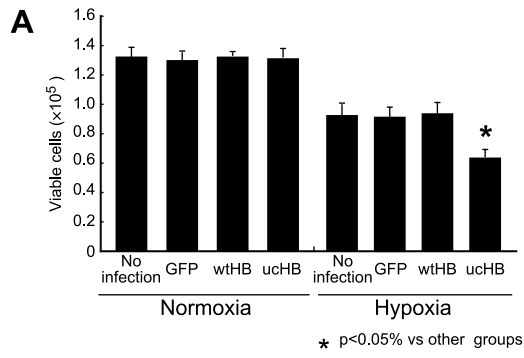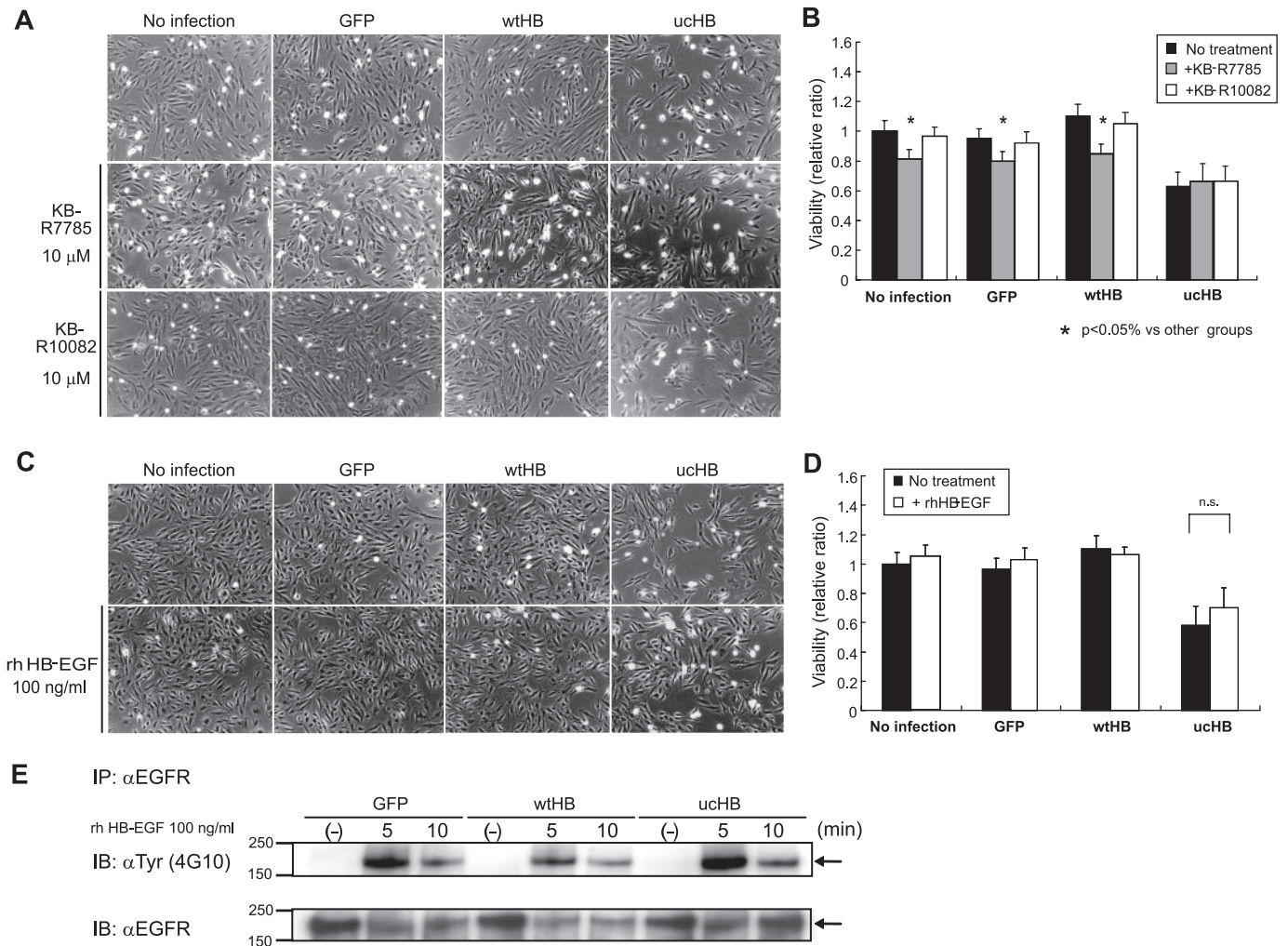
FIGURE 2. **H9c2 cell viability under hypoxic conditions was affected by the addition of ADAM inhibitor, KB-R7785, but it was not restored by the addition of recombinant human HB-EGF (*rhHB-EGF*).** H9c2 cells were incubated under hypoxic conditions for 36 h in the presence of KB-R7785, or KB-R100082 (10 μM) (*A* and *B*), and rhHB-EGF (100 ng/ml) (*C* and *D*). *A* and *C*, representative microscopic images are shown. *B* and *D*, the level of cell viability was determined by a trypan blue dye-exclusion assay. The values (mean $\pm$ S.E.) are representative of three independent experiments. *E*, detection of HB-EGF stimulation through the EGF receptor by an immunoprecipitation (*IP*)-Western blotting assay. Each examination was independently repeated 3 times. *n.s.*, not statistically significant; *IB*, immunoblot.

4, *A* and *B*). Furthermore, we investigated the effect of a ROS scavenger on uc-proHB-EGF/H9c2 apoptosis under hypoxic conditions. Pretreatment with antioxidant NAC significantly reduced the uc-proHB-EGF/H9c2 apoptosis under hypoxic conditions (Fig. 4, *C* and *D*). These data suggest that apoptosis in uc-proHB-EGF/H9c2 under hypoxia are also due to the excessive accumulation of ROS.

Activation of Stress-activated Kinase JNK Signaling Was Involved in Uc-proHB-EGF/H9c2 Apoptosis under Hypoxic

Conditions—During apoptosis, ROS stimulates stress-activated protein kinases such as JNK and p38 via apoptosis signal-regulating kinase 1 (ASK1) (29). To investigate whether the activities of stress signaling pathways are up-regulated in uc-proHB-EGF/H9c2, an immunoblot analysis was performed with an anti-phosphorylated JNK or an anti-phosphorylated p38 antibody. Until 12 h of subjection to hypoxic conditions, no difference was observed in the extent of JNK and p38 phosphorylation among the cells of all groups. However, at 18 h, JNK

FIGURE 1. **Hypoxia-induced apoptosis in H9c2 cells was enhanced by uc-proHB-EGF.** The H9c2 cells transiently expressing GFP, wt-proHB-EGF, and uc-proHB-EGF were incubated under normoxic and hypoxic conditions after adenovirus infection at a multiplicity of infection of 40. *A*, cell viability after 36 h of normoxic and hypoxic conditions was measured by a trypan blue dye-exclusion assay. *B*, representative microscope images after 48 h of infection under normoxic conditions are shown. Nuclear staining was performed using Hoechst 33342. *C*, representative microscope images after 36 h of hypoxic conditions are shown. Nuclear staining was performed using Hoechst 33342. *D*, hypoxia-induced cell death was determined by a trypan blue dye-exclusion assay. Quantitative assays of apoptotic cells (*E* and *F*) (*upper panels*, TUNEL; *lower panels*, Annexin V-FITC) were performed, as described under "Experimental Procedures." *E*, representative immunofluorescent microscopic images are shown. *F*, the number of TUNEL- or Annexin V-FITC-positive cells was counted in 4 fields per well for each experiment. *G*, the effect of co-expression of wt-proHB-EGF on uc-proHB-EGF-enhanced apoptosis is shown. The apoptosis in uc-proHB-EGF/H9c2 cells is indicated as 100%. *H*, hypoxic culture was performed with the H9c2 cells treated by siRNA against *Hb-egf* (HB-EGF siRNA). Apoptosis of the H9c2 cells treated with control siRNA is indicated as 100%. The *inset* shows the knockdown efficiency of HB-EGF siRNA. *cont siRNA*, nonspecific siRNA. The values (mean $\pm$ S.E.) are representative of three independent experiments. *n.s.*, not statistically significant.
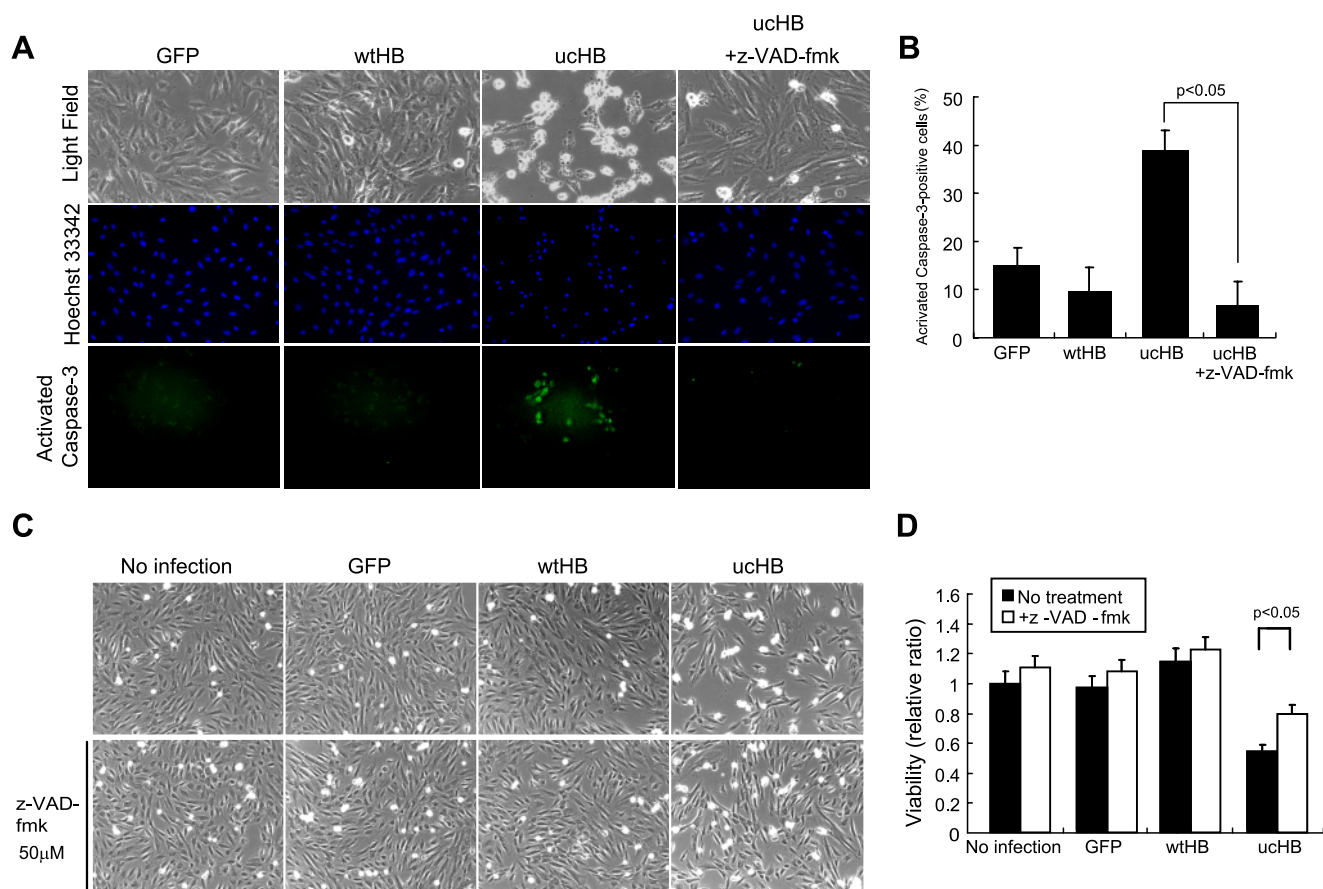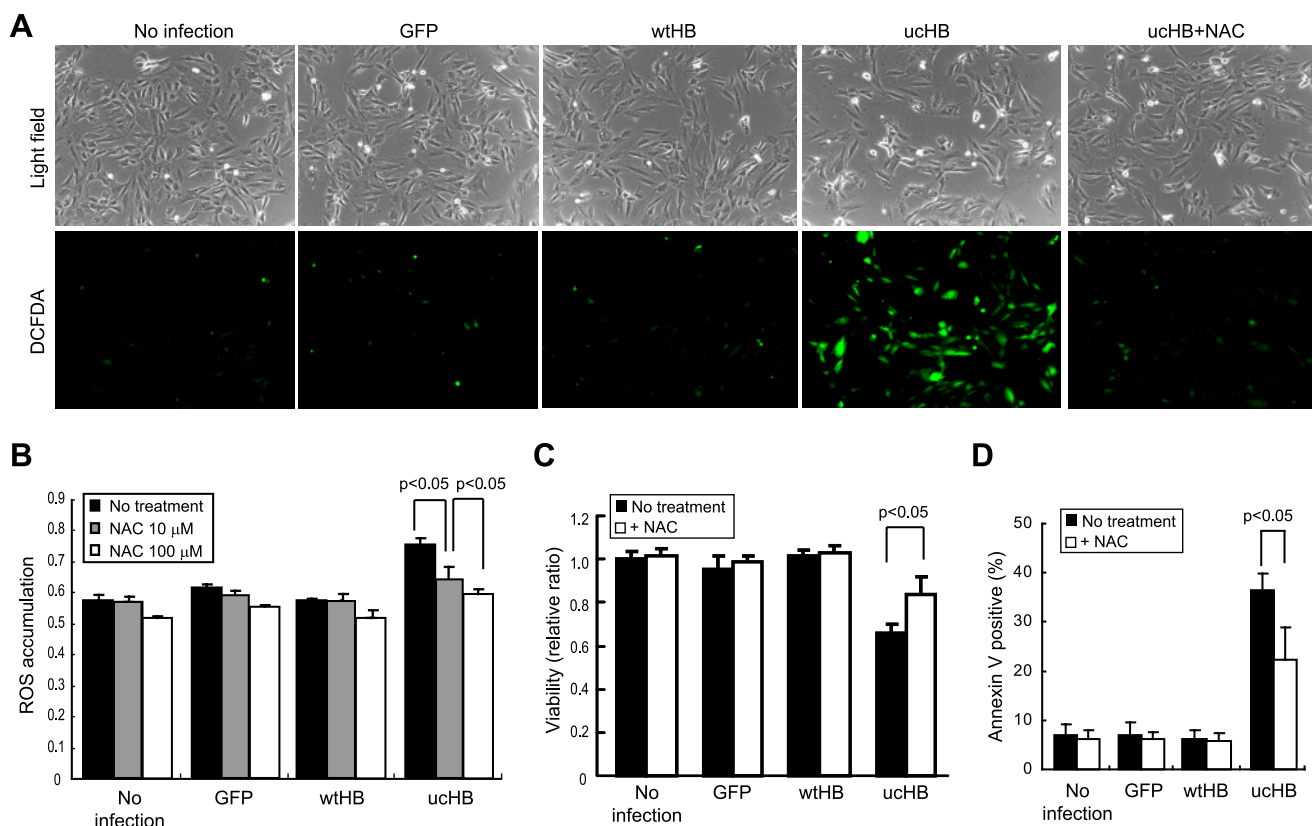
FIGURE 3. **H9c2 cell apoptosis under hypoxic conditions was affected by the addition of a pan-Caspase inhibitor, Z-VAD-fmk.** *A* and *B*, Caspase-3 activity in the H9c2 cells subjected to hypoxic conditions for 36 h was measured using an Apo Logix assay kit. *A*, representative immunofluorescent microscopic images are shown. *B*, the number of the activated Caspase-3 cells was counted in 4 fields per well for each experiment. *C* and *D*, the H9c2 cells were cultured under hypoxic conditions for 36 h in the presence of Z-VAD-fmk (50 μM). *C*, representative microscopic images are shown. *D*, the level of cell survival was determined by a trypan blue dye-exclusion assay. The values (mean ± S.E.) are representative of three independent experiments.

activation markedly increased in uc-proHB-EGF/H9c2 (Fig. 5*A*). Moreover, the inhibition of JNK activity by SP600125, a JNK inhibitor, abrogated uc-proHB-EGF/H9c2 apoptosis under hypoxic conditions (Fig. 5, *B–D*). Activation of Akt and ERK1/2 has also been known to participate in cell survival. We investigated any changes of their activation in transfectants under hypoxic conditions. However, no remarkable difference was observed in the activities of both Akt and ERK1/2 between the wt-proHB-EGF and uc-proHB/H9c2 (Fig. 5*A*). Furthermore, we investigated whether combinational treatments of a pan-Caspase inhibitor, a ROS scavenger, and a JNK inhibitor considerably affect the enhanced uc-proHB-EGF/H9c2 apoptosis under hypoxic conditions. A treatment of Z-VAD-fmk and SP600125 or NAC strongly inhibited uc-proHB-EGF/H9c2 cell apoptosis as compared with each single treatment (Fig. 5*E*). However, the effect of a treatment of these three inhibitors together on apoptosis was similar to that with Z-VAD-fmk and SP600125. On the other hand, these inhibitors did not affect apoptosis of wt-proHB-EGF/H9c2 (data not shown). To confirm that Caspase-3 and JNK are responsible for the apoptosis, a gene knockdown assay was also performed. The protein levels of Caspase-3 or JNK were significantly reduced in each siRNA-treated cells (supplemental Fig. S3*A*). We found that knockdown of Caspase-3 or JNK significantly rescued apoptosis of uc-proHB-EGF/H9c2 (Fig. 5*F*). These data show that both

Caspase- and JNK-dependent pathways, including stimulation by ROS accumulation, mainly work in the apoptosis of uc-proHB-EGF/H9c2.

Expression of XIAP and Bcl-XL Decreased and That of Bax Increased in Uc-proHB-EGF/H9c2 under Hypoxic Conditions— It has been recently shown that HB-EGF-CTF, a product by proHB-EGF shedding, regulates gene transcription via the release of transcriptional repressors from DNA (18, 19). In this study, we examined whether uc-proHB-EGF affects gene expression under hypoxic conditions. By screening apoptosis-related gene expression using RT[2] Profiler PCR array (Super-Array Bioscience), we found that *XIAP* and *Bcl-XL* mRNA decreased, and the expression of *Bax* increased significantly in uc-proHB-EGF/H9c2 after 12 h of subjection to hypoxic conditions (data not shown). Moreover, when quantitative reverse transcriptase-PCR was independently performed using RNA in each group, the expression of *XIAP* and *Bcl-XL* significantly decreased to 20 and 50%, respectively, in uc-proHB-EGF/H9c2 as compared with other groups (Fig. 6*A*, the *left* and *middle panels*). However, the protein level of XIAP, but not Bcl-XL was clearly reduced in uc-proHB-EGF/H9c2 at 24 h after subjection to hypoxic conditions (Fig. 6*B*). In contrast, uc-proHB-EGF/H9c2 provided a 2-fold increase in expression of the *Bax* gene as compared with other groups (Fig. 6*A*, *right panel*). The protein level of Bax in uc-proHB-

FIGURE 4. ROS accumulation significantly increased in uc-proHB-EGF/H9c2 under hypoxic conditions and a ROS scavenger rescued the cells from apoptosis. *A* and *B*, the H9c2 cells subjected to hypoxic conditions for 24 h in the absence or presence of a ROS scavenger, NAC (100 μM), were cultured in fresh medium including DCFDA (20 μM) for 45 min. *A*, representative fluorescent microscopic images are shown. *B*, DCF fluorescence was quantified using a microplate reader; the analysis results are shown. *C*, the level of cell survival was determined by a trypan blue dye-exclusion assay. *D*, apoptotic cells were quantified using an Annexin V-FITC assay as described under "Experimental Procedures." The number of Annexin V-FITC-positive cells was counted in 4 fields per well for each experiment. The values (mean ± S.E.) are representative of three independent experiments.

EGF/H9c2 also increased from 12 h under hypoxia (Fig. 6*B*). These data suggest that the expression pattern of antiapoptotic and proapoptotic genes is altered such that they affect survival in uc-proHB-EGF/H9c2.

DISCUSSION

In this report, we found that overexpression of uc-proHB-EGF caused an enhancement of H9c2 cell apoptosis under hypoxic conditions. Furthermore, metalloproteases inhibitors also enhanced hypoxic cell death of H9c2 cells (Fig. 2, *A* and *B*). On the other hand, knockdown of *Hb-egf* did not enhance the cell death of H9c2 cells under hypoxia (Fig. 1*H*). Previous reports also showed that the cardiomyocytes in *Hb-egf*-null mice are not led to cell death, unlike those in *uc-proHB-EGF* knock-in mice (20, 21). In human trophoblasts, proHB-EGF shedding has been known to be required for survival under hypoxic conditions (11). Therefore, the events of proHB-EGF shedding but not the presence of proHB-EGF are essential for cardiomyocyte survival under hypoxia.

We have previously shown that uc-proHB-EGF, which functions as a dominant negative gene product, is involved in the proliferation of mouse embryonic fibroblasts (30). In this study, we also found co-expression of wt-proHB-EGF did not rescue the cell death of uc-proHB-EGF/H9c2 (Fig. 1*G*). Uc-proHB-EGF mutant is speculated to be useful for analyzing the various effects of a dominant negative modulator on proHB-EGF shedding.

Both HB-EGF and HB-EGF-CTF are released from proHB-EGF by ectodomain shedding. In our study, HB-EGF could not restore the cells from uc-proHB-EGF-enhanced apoptosis (Fig. 2, *C* and *D*). These data indicate that the production of HB-EGF is not involved in the uc-proHB-EGF/H9c2 apoptosis under hypoxic conditions. On the other hand, some novel functions of HB-EGF-CTF have recently been highlighted. After proHB-EGF shedding, HB-EGF-CTF is generated and retrogradely translocated to the inner nuclear membrane (17). HB-EGF-CTF has also been known to regulate the transcriptional level of *cyclin A* and *cyclin D2* by binding to and releasing promyelocytic leukemia zinc finger or Bcl-6 transcriptional repressor from each promoter (18, 19). We have also reported that the induction of c-*Myc* by growth factors is reduced in uc-proHB-EGF-expressing mouse embryonic fibroblasts (30). We thought that the enhancement of the apoptosis may also be due to the events occurring via inadequate transcriptional regulation by insufficient production of HB-EGF-CTF under hypoxia (supplemental Fig. S3*B*). In this study, we performed a gene expression analysis with uc-proHB-EGF/H9c2 under hypoxic conditions, and the expression of *XIAP* was observed to be downregulated (Fig. 6*A*). The level of XIAP protein also decreased in uc-proHB-EGF/H9c2 (Fig. 6*B*). XIAP is a direct inhibitor of Caspases (31). It has recently been reported that XIAP binds to transforming growth factor-β-activated kinase 1 (TAK1) and
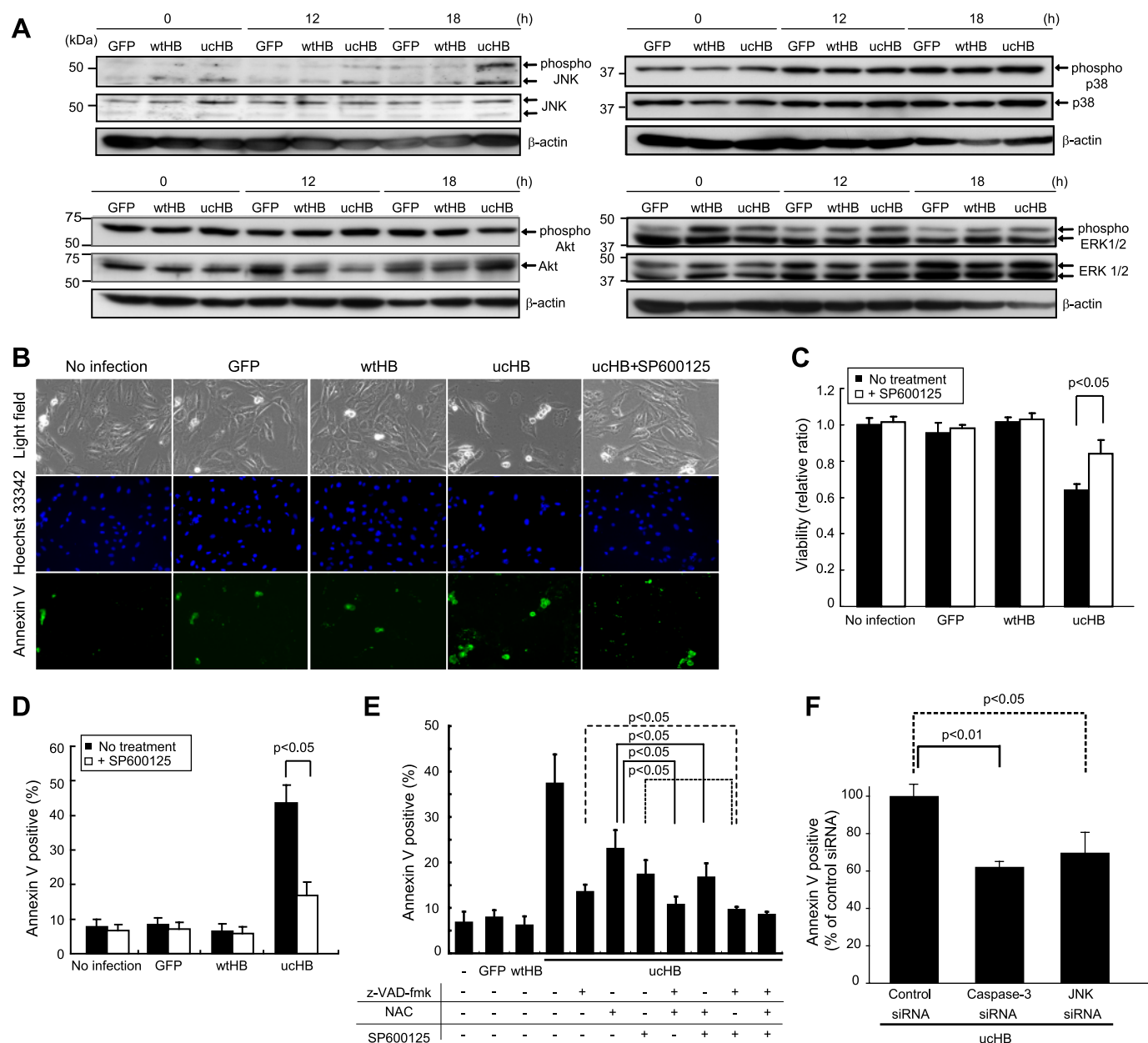
FIGURE 5. **Activation of stress-activated protein kinase in uc-proHB-EGF/H9c2 cells under hypoxic conditions.** *A,* phosphorylation of mitogen-activated protein kinase or phosphatidylinositol 3-kinase was assessed by Western blot analysis using antibodies against phospho-JNK, p38, ERK 1/2, and Akt. *B–D,* H9c2 cells were cultured under hypoxic conditions for 24 h in the absence or presence of a JNK inhibitor, SP600125 (10 μM). *B,* representative microscopic images are shown. *C,* the level of cell survival was determined by a trypan blue dye-exclusion assay. *D,* apoptotic cells were quantified by an Annexin V-FITC assay as described under "Experimental Procedures." The number of Annexin V-FITC-positive cells was counted using 4 fields per well for each experiment. The values (mean $\pm$ S.E.) are representative of three independent experiments. *E,* combinational treatments of the inhibitors were performed to observe the rescue of uc-proHB-EGF/H9c2 from apoptosis. Apoptosis was quantitatively determined by Annexin V-FITC staining. *F,* the effects of Caspase-3 or JNK knockdown in uc-proHB-EGF/H9c2 on hypoxic cell death are represented. Apoptosis of control siRNA-treated uc-proHB-EGF/H9c2 is indicated as 100%. Each experiment was independently performed 3 times.

inhibits the kinase activity of TAK1 toward JNK (32, 33). In this report, the activation of both Caspase-3 and JNK significantly increased in uc-proHB-EGF/H9c2 (Figs. 3, *A* and *B,* and 5*A*). The down-regulation of XIAP could cause an increase in Caspase-3 and JNK activities during hypoxic death of uc-HB-EGF/H9c2. We also detected a down-regulation of Bcl-XL and an up-regulation of Bax in uc-HB-EGF/H9c2 under hypoxic conditions (Fig. 6*A*). Bcl-XL and Bax are members of the Bcl-2 family. Bax increases the permeability of the mitochondrial outer membrane and facilitates the release of cytochrome *c.* The released cytochrome *c* activates Caspase-9, an activator of Caspase-3. Bcl-XL binds to Bax to inhibit apoptosis (34). The expression pattern of the Bcl-2 family members observed in uc-proHB-EGF/H9c2 indicates that the cells might be in a proapoptotic state due to increased mitochondrial membrane permeability. We advocate that impairment shedding of proHB-EGF in hypoxia reduces a threshold level of Caspase-3 and JNK activation via gene regulation of *XIAP* and the *Bcl-2* family members, and leads to cell death (Fig. 7).
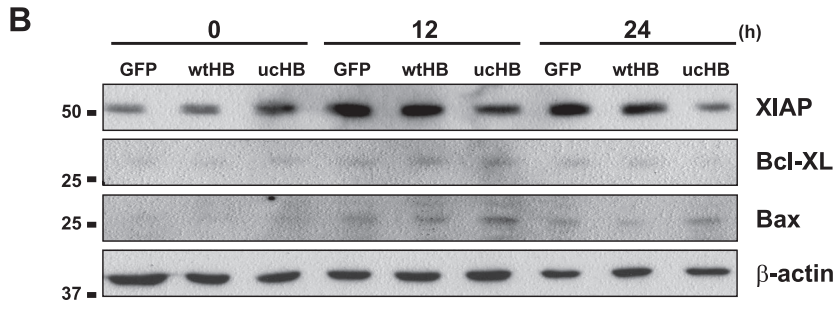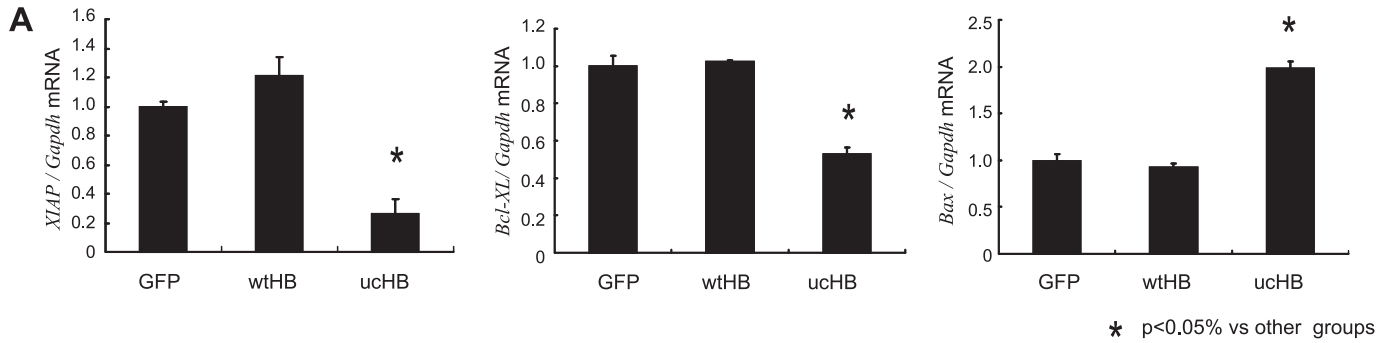
A

* p<0.05% vs other groups

B

FIGURE 6. **The expression of antiapoptotic and proapoptotic molecules was altered in uc-proHB-EGF/H9c2.** *A*, the expression levels of *XIAP*, *Bcl-XL*, and *Bax* mRNAs in GFP/H9c2, wt proHB-EGF/H9c2, and uc-proHB-EGF/H9c2 cells were assessed by quantitative real-time PCR. Each sample was collected at 12 h after subjection of the cells to hypoxic conditions. *B*, the levels of XIAP, Bcl-XL, and Bax protein are represented at each indicated time after hypoxia by Western blot analysis. *β*-Actin serves as a loading control.
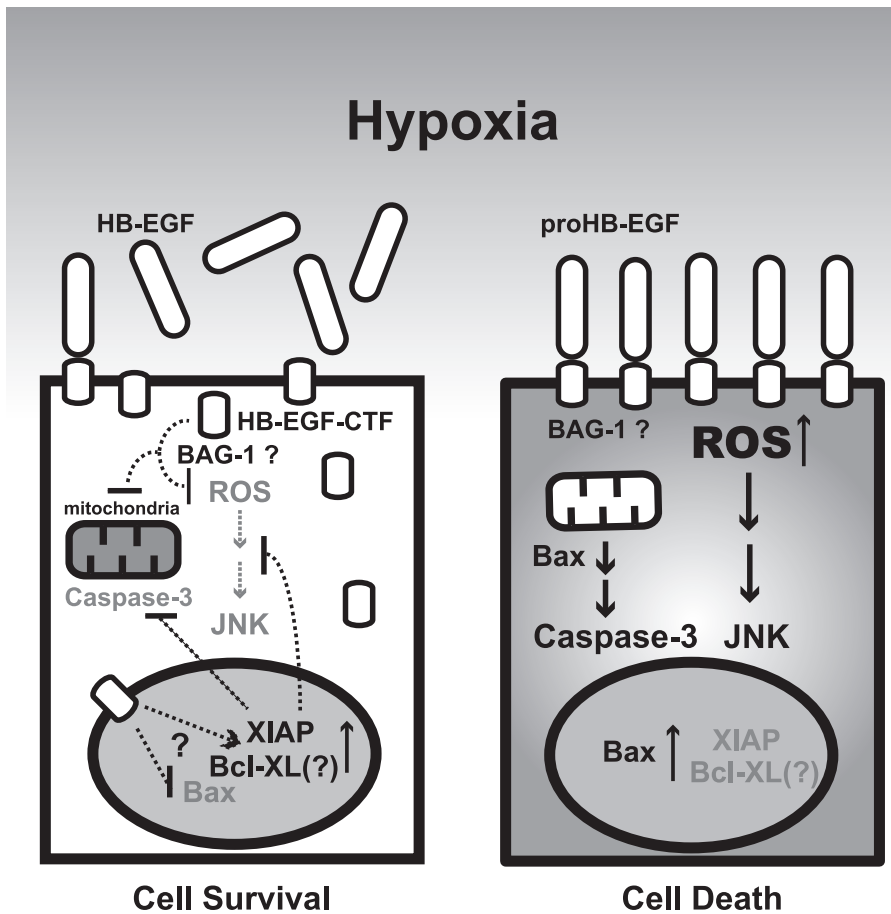

FIGURE 7. **Representation of a molecular mechanism underlying cardiomyocyte death due to insufficient proHB-EGF shedding under hypoxia.**

The cytoplasmic domain of proHB-EGF has also been reported to bind Bcl-2-associated athanogene (BAG-1), and the interaction of BAG-1 with a proHB-EGF molecule leads to decreased cell adhesion and increased cell viability with etoposide treatment (35). BAG-1 functions as an antiapoptotic factor when associated with Bcl-2 (36, 37). BAG-1 also associates with heat shock protein-70, which is a heat shock transcription factor-1-induced cell protector (38). However, it still remains unknown whether HB-EGF-CTF forms a complex with BAG-1 and regulates the antiapoptotic functions. Further examinations are required to elucidate the relationship between the involvement of uc-proHB-EGF and BAG-1 in hypoxic cell death. We unveiled that ROS accumulated in uc-proHB-EGF/H9c2 under hypoxic conditions (Fig. 4, *A* and *B*) and that a ROS scavenger rescued uc-proHB-EGF/H9c2 from the apoptosis under hypoxic conditions. BAG-1 has been also known to act as an antioxidant (37). The above-mentioned data suggest that proHB-EGF shedding could also

control BAG-1 to regulate redox reactions by retaining a reducing intracellular environment.

As a conflicting data, Krieg *et al.* (39) reported that proHB-EGF shedding generated ROS following EGF receptor transactivation. They used chemical components such as acetylcholine to mimic an ischemic preconditioning state. We used rat-derived cells in this study, whereas Krieg *et al.* (39) studied with rabbit-derived cells. These differences could lead to the distinct results. However, our data are consistent with the *in vivo* data (20, 21). It has been recently reported that oxidative stress increases in patients with idiopathic cardiomyopathy or idiopathic dilated cardiomyopathy (40). A uc-proHB-EGF knock-in mouse exhibited a similar condition in idiopathic cardiomyopathy or idiopathic dilated cardiomyopathy (21). Insufficient shedding of proHB-EGF could play a role in increasing oxidative stress in these disorders.

It has been established that the accumulation of ROS induces JNK activation via the activation of ASK1 (29, 41) and ASK1 knock-out neonatal cardiomyocytes are resistant to H_2O_2-induced apoptosis (42). On the basis of the above reports, it may be assumed that ROS-ASK1 signaling stimulated JNK in our study. On the other hand, the combination of NAC and SP600125 was more effective in the survival of uc-proHB-EGF/H9c2 cells than a treatment of NAC alone (Fig. 5*E*). This indicates that there are other stimulators of JNK activation besides ROS.

In this study, we demonstrated that uc-proHB-EGF enhanced induction of apoptosis under hypoxic conditions. Thus, we can assume that disruption of proHB-EGF shedding could lead to extensive cardiomyocyte apoptosis and poor prognosis in patients with ischemic heart disease, who are exposed to excessive hypoxic stress. This raises the possibilities that the amount of HB-EGF in the heart is a marker of prognosis in patients with ischemic heart disease and that improving insufficient shedding of proHB-EGF might develop as a new therapeutic strategy for cardiac disorder.

REFERENCES

1. Higashiyama, S., Abraham, J. A., Miller, J., Fiddes, J. C., and Klagsbrun, M. (1991) *Science* **251,** 936–939
2. Perrella, M. A., Maki, T., Prasad, S., Pimental, D., Singh, K., Takahashi, N., Yoshizumi, M., Alali, A., Higashiyama, S., and Kelly, R. A. (1994) *J. Biol. Chem.* **269,** 27045–27050
3. Feng, J., Mehta, V. B., El-Assal, O. N., Wu, D., and Besner, G. E. (2006) *Peptides* **27,** 1589–1596
4. Pillai, S. B., Turman, M. A., and Besner, G. E. (1998) *J. Pediatr. Surg.* **33,** 973–978; Discussion, 978–979
5. Pillai, S. B., Hinman, C. E., Luquette, M. H., Nowicki, P. T., and Besner, G. E. (1999) *J. Surg. Res.* **87,** 225–231
6. Sakai, M., Tsukada, T., and Harris, R. C. (2001) *Exp. Nephrol.* **9,** 28–39
7. Homma, T., Sakai, M., Cheng, H. F., Yasuda, T., Coffey, R. J., Jr., and Harris, R. C. (1995) *J. Clin. Investig.* **96,** 1018–1025
8. Horikawa, M., Higashiyama, S., Nomura, S., Kitamura, Y., Ishikawa, M., and Taniguchi, N. (1999) *FEBS Lett.* **459,** 100–104
9. Tanaka, N., Sasahara, M., Ohno, M., Higashiyama, S., Hayase, Y., and Shimada, M. (1999) *Brain Res.* **827,** 130–138
10. Jin, K., Mao, X. O., Sun, Y., Xie, L., Jin, L., Nishi, E., Klagsbrun, M., and Greenberg, D. A. (2002) *J. Neurosci.* **22,** 5365–5373
11. Armant, D. R., Kilburn, B. A., Petkova, A., Edwin, S. S., Duniec-Dmuchowski, Z. M., Edwards, H. J., Romero, R., and Leach, R. E. (2006) *Development* **133,** 751–759
12. Ushikoshi, H., Takahashi, T., Chen, X., Khai, N. C., Esaki, M., Goto, K., Takemura, G., Maruyama, R., Minatoguchi, S., Fujiwara, T., Nagano, S., Yuge, K., Kawai, T., Murofushi, Y., Fujiwara, H., and Kosai, K. (2005) *Lab. Investig.* **85,** 862–873
13. Iwabu, A., Murakami, T., Kusachi, S., Nakamura, K., Takemoto, S., Komatsubara, I., Sezaki, S., Hayashi, J., Ninomiya, Y., and Tsuji, T. (2002) *Basic Res. Cardiol.* **97,** 214–222
14. Tanaka, N., Masamura, K., Yoshida, M., Kato, M., Kawai, Y., and Miyamori, I. (2002) *Biochem. Biophys. Res. Commun.* **297,** 375–381
15. Higashiyama, S., and Nanba, D. (2005) *Biochim. Biophys. Acta* **1751,** 110–117
16. Higashiyama, S., Iwabuki, H., Morimoto, C., Hieda, M., Inoue, H., and Matsushita, N. (2008) *Cancer Sci.* **99,** 214–220
17. Hieda, M., Isokane, M., Koizumi, M., Higashi, C., Tachibana, T., Shudou, M., Taguchi, T., Hieda, Y., and Higashiyama, S. (2008) *J. Cell Biol.* **180,** 763–769
18. Kinugasa, Y., Hieda, M., Hori, M., and Higashiyama, S. (2007) *J. Biol. Chem.* **282,** 14797–14806
19. Nanba, D., Mammoto, A., Hashimoto, K., and Higashiyama, S. (2003) *J. Cell Biol.* **163,** 489–502
20. Iwamoto, R., Yamazaki, S., Asakura, M., Takashima, S., Hasuwa, H., Miyado, K., Adachi, S., Kitakaze, M., Hashimoto, K., Raab, G., Nanba, D., Higashiyama, S., Hori, M., Klagsbrun, M., and Mekada, E. (2003) *Proc. Natl. Acad. Sci. U. S. A.* **100,** 3221–3226
21. Yamazaki, S., Iwamoto, R., Saeki, K., Asakura, M., Takashima, S., Yamazaki, A., Kimura, R., Mizushima, H., Moribe, H., Higashiyama, S., Endoh, M., Kaneda, Y., Takagi, S., Itami, S., Takeda, N., Yamada, G., and Mekada, E. (2003) *J. Cell Biol.* **163,** 469–475
22. Tokumaru, S., Higashiyama, S., Endo, T., Nakagawa, T., Miyagawa, J. I., Yamamori, K., Hanakawa, Y., Ohmoto, H., Yoshino, K., Shirakata, Y., Matsuzawa, Y., Hashimoto, K., and Taniguchi, N. (2000) *J. Cell Biol.* **151,** 209–220
23. Asakura, M., Kitakaze, M., Takashima, S., Liao, Y., Ishikura, F., Yoshinaka, T., Ohmoto, H., Node, K., Yoshino, K., Ishiguro, H., Asanuma, H., Sanada, S., Matsumura, Y., Takeda, H., Beppu, S., Tada, M., Hori, M., and Higashiyama, S. (2002) *Nat. Med.* **8,** 35–40
24. Goishi, K., Higashiyama, S., Klagsbrun, M., Nakano, N., Umata, T., Ishikawa, M., Mekada, E., and Taniguchi, N. (1995) *Mol. Biol. Cell* **6,** 967–980
25. Majander, A., Finel, M., and Wikstrom, M. (1994) *J. Biol. Chem.* **269,** 21037–21042
26. Chandel, N. S., Maltepe, E., Goldwasser, E., Mathieu, C. E., Simon, M. C., and Schumacker, P. T. (1998) *Proc. Natl. Acad. Sci. U. S. A.* **95,** 11715–11720
27. Chandel, N. S., McClintock, D. S., Feliciano, C. E., Wood, T. M., Melendez, J. A., Rodriguez, A. M., and Schumacker, P. T. (2000) *J. Biol. Chem.* **275,** 25130–25138
28. Guzy, R. D., Hoyos, B., Robin, E., Chen, H., Liu, L., Mansfield, K. D., Simon, M. C., Hammerling, U., and Schumacker, P. T. (2005) *Cell Metab.* **1,** 401–408
29. Tobiume, K., Matsuzawa, A., Takahashi, T., Nishitoh, H., Morita, K., Takeda, K., Minowa, O., Miyazono, K., Noda, T., and Ichijo, H. (2001) *EMBO Rep.* **2,** 222–228
30. Nanba, D., Inoue, H., Shigemi, Y., Shirakata, Y., Hashimoto, K., and Higashiyama, S. (2008) *J. Cell Physiol.* **214,** 465–473
31. Deveraux, Q. L., Takahashi, R., Salvesen, G. S., and Reed, J. C. (1997) *Nature* **388,** 300–304
32. Sanna, M. G., da Silva Correia, J., Ducrey, O., Lee, J., Nomoto, K., Schrantz, N., Deveraux, Q. L., and Ulevitch, R. J. (2002) *Mol. Cell. Biol.* **22,** 1754–1766
33. Kaur, S., Wang, F., Venkatraman, M., and Arsura, M. (2005) *J. Biol. Chem.* **280,** 38599–38608

34. Youle, R. J., and Strasser, A. (2008) *Nat. Rev. Mol. Cell Biol.* **9,** 47–59
35. Lin, J., Hutchinson, L., Gaston, S. M., Raab, G., and Freeman, M. R. (2001) *J. Biol. Chem.* **276,** 30127–30132
36. Takayama, S., Sato, T., Krajewski, S., Kochel, K., Irie, S., Millan, J. A., and Reed, J. C. (1995) *Cell* **80,** 279–284
37. Schulz, J. B., Bremen, D., Reed, J. C., Lommatzsch, J., Takayama, S., Wullner, U., Loschmann, P. A., Klockgether, T., and Weller, M. (1997) *J. Neurochem.* **69,** 2075–2086
38. Takayama, S., Bimston, D. N., Matsuzawa, S., Freeman, B. C., Aime-Sempe, C., Xie, Z., Morimoto, R. I., and Reed, J. C. (1997) *EMBO J.* **16,** 4887–4896
39. Krieg, T., Cui, L., Qin, Q., Cohen, M. V., and Downey, J. M. (2004) *J. Mol. Cell Cardiol.* **36,** 435–443
40. Yucel, D., Aydogdu, S., Senes, M., Topkaya, B. C., and Nebioglu, S. (2002) *Scand. J. Clin. Lab. Investig.* **62,** 463–468
41. Tobiume, K., Saitoh, M., and Ichijo, H. (2002) *J. Cell. Physiol.* **191,** 95–104
42. Yamaguchi, O., Higuchi, Y., Hirotani, S., Kashiwase, K., Nakayama, H., Hikoso, S., Takeda, T., Watanabe, T., Asahi, M., Taniike, M., Matsumura, Y., Tsujimoto, I., Hongo, K., Kusakari, Y., Kurihara, S., Nishida, K., Ichijo, H., Hori, M., and Otsu, K. (2003) *Proc. Natl. Acad. Sci. U. S. A.* **100,** 15883–15888